Fatigue Substantiation and Damage Tolerance Evaluation of Rotorcraft Horizontal Tail

R Vijaya Kumar
Rotary Wing R&D Center,
Hindustan Aeronautics Limited, Bangalore-560017, India.

Cody Godines[§] and Frank Abdi[§]
[§]Alpha Star Corporation,
5199 E Pacific Coast Hwy, Suite 410,
Long Beach, California 90804, USA

Abstract

To ensure safe operation of the helicopter throughout its lifetime the primary structure has to be designed taking into account damage tolerance criteria. This has been considered in the design process for example by using multiple load paths as well as by taking into account the presence of certain structural defects like impacts or manufacturing defects in composite parts when performing the dimensioning and lifetime calculations. This paper describes and presents an effort performed for Damage Tolerance (DT) aspects of rotorcraft Horizontal Tail (HT) through Multi-Scale (MS) modeling computational approach to assess the growth rate of damages from fatigue under spectrum loading from rotorcraft mission profile and consideration of the effects of material variability to assess structural advantages. Main emphasis was laid on the design of the cyclic loaded components in order to achieve unlimited life with high flaw tolerance. A micromechanics based Multi-Scale Progressive Failure Analysis (MS-PFA) approach that detects damage and fracture evolution is carried out to assess the Durability and Damage Tolerance (D&DT) of HT with effect of defects: 1) ply-drop-off, and features at the reduced skin thicknesses along the length of spar; 2) fiber waviness exhibited in thick sections; and 3) void shape, size, distribution. Fatigue life is estimated under service spectrum block loading conditions in critical mission by determining the material stiffness and strength degradation, failure load and cycles.

Keywords: Horizontal Tail, Spectrum loading, Fatigue Life, Ply drop-off, Damage Accumulation, Durability, Damage Tolerance

1 INTRODUCTION

Fatigue analysis can be considered as low, high, and two-staged (load sequence sensitive) cycles under quasi static, harmonic, and Power Spectral Density (PSD) loading. Certification authorities demand for an improved damage tolerant behaviour, especially for dynamically loaded structures. The outstanding fatigue tolerance features of composite structures were the reason for introducing composite rotor blades and composite fuselage in the helicopter design. An important issue for such structural applications is the long-term behavior and/or durability of the fiber-reinforced composite materials. Composite structures are often subjected to dynamic loading caused by forced vibrations. For this reason it is desirable to have a computational tool that provides an accurate analysis of composite structures under cyclic loading conditions. During fatigue, after every cyclic loading, the failure criteria and failure modes will be checked with composite mechanics module, damage will cause a degradation of the constituent material properties, the degradation of each layer will be stored, the structural model will be updated with the degraded material properties and fractured nodes/elements will be removed. Once damage stops to progress at a given cycle, equilibrium is reached and the next cycle of fatigue will occur. If damage is spreading the same cycle is run with the new damage until the damage stops spreading. Damage equilibrium must occur before continuing to the next cycle.

Painstaking and systematic research by Wöhler [1], the superintendent of a railway depot in Prussia, established a systematic relationship between the magnitude of periodic loads applied on a specimen and the number of cycles to its failure. More significantly, Wöhler determined that there is a certain minimum magnitude of cyclic loading below which the material will withstand seemingly infinite cycling. This stress amplitude is termed the fatigue limit. Thus a material constant was finally available in order to design for durability. Wöhler established that the fatigue limit is extremely sensitive to mean stress. The new rule for the helicopter design considering fatigue and damage tolerance (“Damage Tolerance and Fatigue Evaluation of Composite Rotorcraft Structures”, FAR 27/29 §573) was introduced in 2010 [2].

One of the first applications of fiber reinforced composites in rotorcraft has been composite fuselage and rotor blades. In 1967, the BO105 a product of the former helicopter division of MBB, afterwards EUROCOPTER Deutschland GmbH, now Airbus Helicopters, flew for the first time with full composite main and tail rotor blades. Later on BK117, EC135 helicopters followed to extend the usage of composites from secondary parts such as fairings to primary fuselage structures. In the 90s the certification authorities and the helicopter industry developed a new fatigue and damage tolerance approach. The complicate design of the complete rotor blade with fatigue and damage tolerance approach is described by Bansemir et al. [3,4].

India's Hindustan Aeronautics Limited (HAL) is launched a multipurpose twin engine HAL Dhruv (first flight in 1992) is a utility helicopter with hinge less rotor system is developed and manufactured to meet the requirement of both military and civil operators, with military variants of the helicopter being developed for the Indian Armed Forces, while a variant for civilian/commercial use has also been developed. This helicopter is designed to accommodate up to 7 persons in its aerodynamically shaped fuselage and has some unique features like a bearingless composite main rotor, a Fenestron anti-torque system and an Anti-Resonance Isolation System (ARIS). As a modem helicopter it offers state-of-the-art safety features like crashworthiness and damage tolerant layout and takes advantage of the latest design technology. The development of attack Light Combat Helicopter (LCH) (first flight in 2010) is carried out with the same rotor system. Both helicopters are certified according to Federal aviation requirements FAR 29 under Category A.

Damage tolerance criteria became necessary to account for the contribution of individual load cycles in a service load spectrum to cumulative fatigue damage eventually leading to failure. Pålmgren's and then Miner's linear damage accumulation law [5] finally made this possible. However, Gassner [6] established that cyclic damage accumulation is not linear. Depending on the material, the service load spectrum, and the sequence of loads in the given spectrum, the damage sum at failure can vary over a very wide range, in fact by about two orders of magnitude. Very importantly, Gassner also established that for a given combination of material and service load spectra, the damage sum would not vary significantly.

The inhomogeneous and anisotropic properties of fiber-reinforced composite materials make the fatigue analysis more complicated compared to homogeneous and isotropic materials. The fiber-reinforced composite responses to cyclic loading differently mainly due to different types of damages such as matrix cracks, fiber kinks, delaminations, broken fibers, etc. Consequently, a large research effort has been conducted to understand the complex phenomenon of fatigue in composite materials and to predict the behavior aiming to achieve a more efficient design using these material.

In recent years "virtual testing" has increased in use in order to try new materials in structures earlier in an applications timeline. Virtual testing is made possible by conducting progressive failure analysis and combining those results to predict structure/component safety based on the physics and micro/macro mechanics of materials, manufacturing processes, available data, and service environments. The approach takes progressive damage and fracture processes into account and accurately assesses reliability and durability by predicting failure initiation and progression based on constituent material properties. Such approaches are becoming more widespread and economically advantageous in some applications.

2 SIMULATION METHODOLOGY

This section describes a computational simulation approach for durability, damage tolerance (D&DT) and reliability of composite structures in presence of uncertainties in material properties. This computer-based prediction methodology combines composite mechanics with finite element analysis, damage and fracture tracking capability, probabilistic analysis and a robust design algorithm to reduce weight of composite structures without loss in structural durability and reliability.

The fatigue building block predictions validation is performed using ASTM coupon un-notched test data. An approach towards this is shown in Figure 1. Once simulations are accurate enough to predict test, certification by analysis can be achieved or B-Basis allowable can be computed with limited test data.

Objective:	Objective:	OPEN-HOLE (Example Layup)
Predict Resin, Fiber S-N Curves Tests Used: 0^0 Fatigue 90^0 Fatigue Predict: Stress-Cycle Curves (Fiber and Matrix)	Match S-N Curve using MCQ, MS-PFA, and VCCT Tests Used: $\pm 45^0$ Fatigue 90^0 3-Point Bend Fatigue ENF Fatigue DCB Fatigue Analysis: VCCT MS-PFA MCQ	$[+30, +60, 90, -60, -30]_{2S}$ $[+60, 0, -60]_{3S}$ $[0, +45, 90, -45]_{2S}$ Example of Predictions: @ 100K, 200K, 300K Damage type Damage location Damage amount Stiffness Drop Fatigue life at specific stress level Residual Strength after 200K or 300K Tension Compression

Figure 1 Flow Process Fatigue Prediction

Calibration, Verification, Validation, Predictions (Accreditation)

At the start of the fatigue simulations, the static composite material predictions are performed. The fatigue model prediction with commercial code GENOA for MS-PFA is based on damage mechanics theory along with calibrated S-N curve for constituent properties from unidirectional 0˚ and 90˚ fatigue. Details of static and fatigue calibration using ASTM tests on unidirectional coupons as well as the theory and progressive failure analysis methodology is discussed in blind failure predictions [7, 8] for IM7/977-3 Carbon epoxy material system. Structural application is shown in [9], where material characterization of unidirectional Carbon epoxy (NCT307-D1-34-600), a unidirectional E-Glass epoxy (NCT307-D1-E300) and E-Glass epoxy weave (NB307-D1 7781 497A) was performed to reverse engineer the fiber matrix and architecture properties.

The approach was later extended by Galib Abumeri et al. [10,11] to a full composite turbine blade with finite element based multi-scale progressive failure analysis to determine failure modes and locations as well as the fracture load under static loading with sensitivity and reliability computations that reduced weight by 10%. D&DT analysis results were validated with the static test performed at Sandia National Laboratories. The system consisted of Stitched Double Bias Glass (DBM1708), Uni Glass (ELT5500), Balsa, Steel Gelcoat, Chopped Glass Mat (0.75oz), Carbon/Glass Triax, all of which can be calibrated with MCQ software and plugged into various FE codes for Multi Scale Progressive Failure Analysis (MS-PFA). Certification of composite system is performed by performing building block simulation and test correlations beginning with material characterization and ending with substructures and structures.

The progressive damage model in GENOA degrades the constituent laminate properties allowing for root cause failure determination. As we go into details recall that this is a building block approach in which both test and simulation become more mature along the way learning from each other until predictions can be used to reduce test. D&DT of a simulated blade structure is evaluated for tapered laminates with ply drop offs and resin rich areas under static and fatigue loading. Certification of composite system is performed by performing building block simulation and test correlations beginning with material characterization and ending with substructures and structures.

Figure 2 shows the static simulation prediction damage mechanisms and failure zone vs test. The failure load of simulation was 48.29 kN and test was 48.612 kN with both failures occurring at the root of the blade.

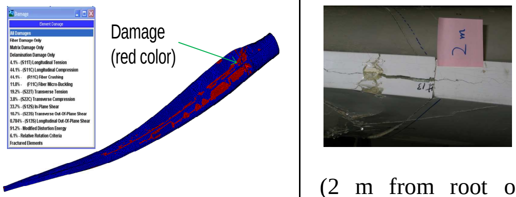

a) Damage at peak load of 48.29KN

(2 m from root of the blade)

b) Damage at test peak load of 48.612KN

Figure 2 Progressive failure analysis and test validation of Sandia's BSDS blade under static loading (Source: Ref. 10)

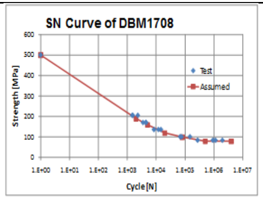

Figure 3 Calibration results of Glass epoxy material vs test

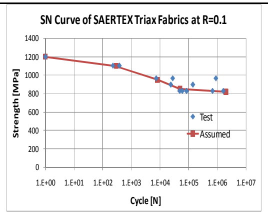

Figure 4 Calibration results of Triaxial Glass Fabric vs test

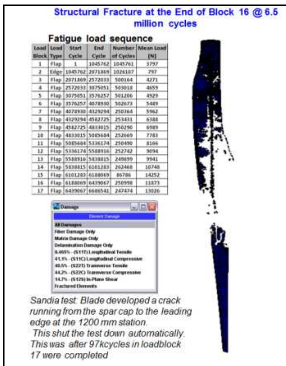
Structural Fracture at the End of Block 16 @ 6.5 million cycles

Fatigue load sequence

Load Block	Load Type	Start Cycle	End Cycle	Number of Cycles	Mean Load (N)
1	Flap	1	1045762	1045761	3797
2	Edge	1045762	2071869	1026107	797
3	Flap	2071869	2572033	500164	4271
4	Flap	2572033	3075051	503018	4659
5	Flap	3075051	3576257	501206	4929
6	Flap	3576257	4078930	502673	5489
7	Flap	4078930	4329294	250364	5962
8	Flap	4329294	4582725	253431	6388
9	Flap	4582725	4833015	250290	6989
10	Flap	4833015	5085684	252669	7783
11	Flap	5085684	5336174	250490	8166
12	Flap	5336174	5588916	252742	9094
13	Flap	5588916	5838815	249899	9941
14	Flap	5838815	6101283	262468	10748
15	Flap	6101283	6188069	86786	14252
16	Flap	6188069	6439067	250998	11873
17	Flap	6439067	6686541	247474	13026

Sandia test: Blade developed a crack running from the spar cap to the leading edge at the 1200 mm station. This shut the test down automatically. This was after 97kcycles in loadblock 17 were completed

Figure 5 Fatigue load blocks, and simulation fatigue results (16 blocks) vs test of 9m wind blade (17 blocks)

0

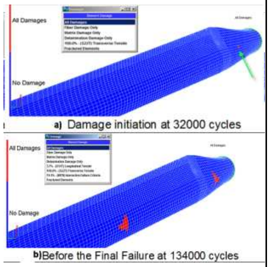

a) Damage initiation at 32000 cycles

b) Before the Final Failure at 134000 cycles

Figure 6 Simulation predictions for 33mm wind blade (a) damage initiation and (b) final failure

The final result of the certification simulations were obtained when fatigue properties were calibrated for the wind blade materials (Figure 3 and Figure 4) and used in spectrum fatigue simulations for a 9 meter wind blade validation with test (Figure 5) and 33 meter wind blade full simulation prediction (Figure 6).

3 DURABILITY AND DAMAGE TOLERANCE EVALUATION OF HORIZONTAL TAIL

In the present work, durability and damage tolerance evaluation of helicopter HT is carried out. The HT was modeled using the ANSYS Composite Prepost (ACP) preprocessor. The input file generated from the ANSYS Workbench is imported into GENOA MS-PFA. The analysis was based on a numerical model of HT to obtain stress fields under defined loads and to estimate fatigue life. In order to do so, the load spectrum was obtained by means of strain gauge measurements during a series of experimental flights. Data collected during flights was post-processed to create a characteristic ten hour spectrum that would statistically represent the flight profile for helicopter. The simulation studies are carried out for fatigue block loading from specified mission profile of helicopter.

Work Flow from ANSYS ACP to GENOA for spectrum analysis is shown in Figure 7.

Figure 7 Work Flow from ANSYS ACP to GENOA

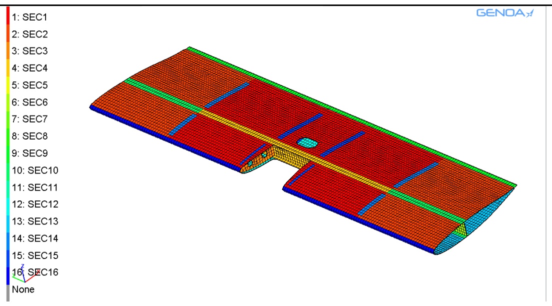

Figure 8 Geometry and layup sections of the HT

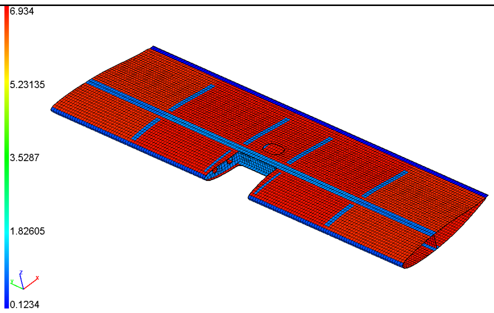

Figure 9 Thickness (mm) plot of sections of HT

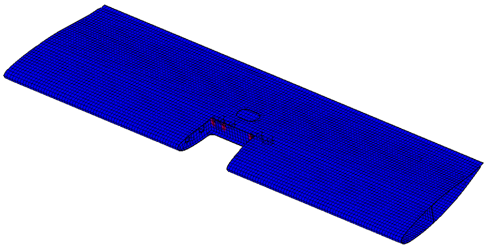

Figure 10 Specified boundary conditions at centre Spar of HT

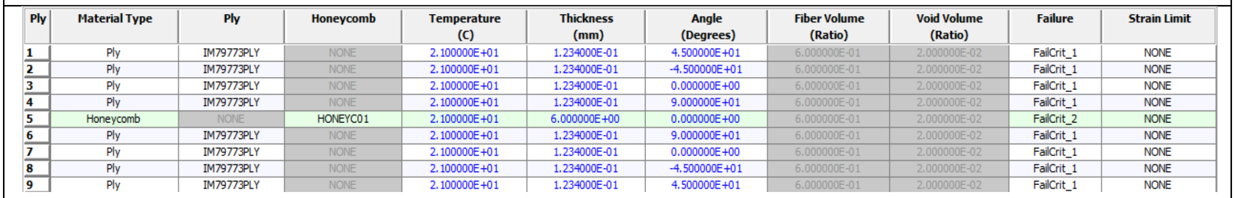

Ply	Material Type	Ply	Honeycomb	Temperature (C)	Thickness (mm)	Angle (Degrees)	Fiber Volume (Ratio)	Void Volume (Ratio)	Failure	Strain Limit
1	Ply	IM79773PLY	NONE	2.100000E+01	1.234000E-01	4.500000E+01	6.000000E-01	2.000000E-02	FailCrit_1	NONE
2	Ply	IM79773PLY	NONE	2.100000E+01	1.234000E-01	-4.500000E+01	6.000000E-01	2.000000E-02	FailCrit_1	NONE
3	Ply	IM79773PLY	NONE	2.100000E+01	1.234000E-01	0.000000E+00	6.000000E-01	2.000000E-02	FailCrit_1	NONE
4	Ply	IM79773PLY	NONE	2.100000E+01	1.234000E-01	9.000000E+01	6.000000E-01	2.000000E-02	FailCrit_1	NONE
5	Honeycomb	NONE	HONEYC01	2.100000E+01	6.000000E+00	0.000000E+00	6.000000E-01	2.000000E-02	FailCrit_2	NONE
6	Ply	IM79773PLY	NONE	2.100000E+01	1.234000E-01	9.000000E+01	6.000000E-01	2.000000E-02	FailCrit_1	NONE
7	Ply	IM79773PLY	NONE	2.100000E+01	1.234000E-01	0.000000E+00	6.000000E-01	2.000000E-02	FailCrit_1	NONE
8	Ply	IM79773PLY	NONE	2.100000E+01	1.234000E-01	-4.500000E+01	6.000000E-01	2.000000E-02	FailCrit_1	NONE
9	Ply	IM79773PLY	NONE	2.100000E+01	1.234000E-01	4.500000E+01	6.000000E-01	2.000000E-02	FailCrit_1	NONE

Figure 11 Layup details of section 7

The specified boundary conditions at the center of the HT are shown in Figure 10. The translations in x, y and z directions are arrested. The zone with the boundary was held from being damaged to prevent premature failure due to boundary condition affects. The model consists of centre spar with ribs and sandwich made top and bottom shells which are bonded together. The carbon epoxy and honeycomb materials are used. The layups vary across the geometry. One of the layups with honeycomb which represents sandwich panel is shown in Figure 11.

The IM79773 carbon epoxy prepreg fiber and matrix properties are shown in Figure 12, Figure 13 and Figure 14. The honeycomb properties are shown in Figure 5. The SN curves [2] for the fiber and matrix are shown in Figure 16 and Figure 17. The honeycomb SN curve is assumed and goes from the static strength to 75% of static strength at 1e06 cycles and then drops to a lower value.

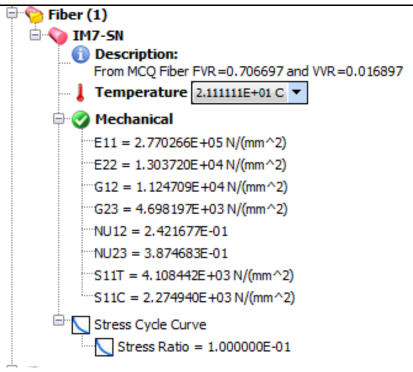

Fiber (1)
IM7-SN
Description:
From MCQ Fiber FVR=0.706697 and VVR=0.016897
Temperature 2.111111E+01 C
Mechanical
E11 = 2.770266E+05 N/(mm^2)
E22 = 1.303720E+04 N/(mm^2)
G12 = 1.124709E+04 N/(mm^2)
G23 = 4.698197E+03 N/(mm^2)
NU12 = 2.421677E-01
NU23 = 3.874683E-01
S11T = 4.108442E+03 N/(mm^2)
S11C = 2.274940E+03 N/(mm^2)
Stress Cycle Curve
Stress Ratio = 1.000000E-01

Figure 12 Linear Fiber Properties

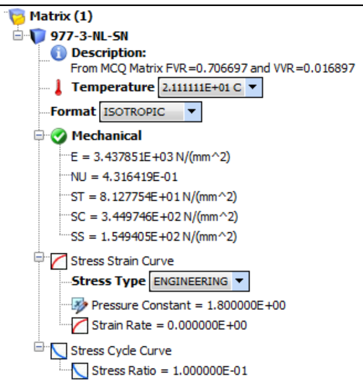

Matrix (1)
977-3-NL-SN
Description:
From MCQ Matrix FVR=0.706697 and VVR=0.016897
Temperature 2.111111E+01 C
Format ISOTROPIC
Mechanical
E = 3.437851E+03 N/(mm^2)
NU = 4.316419E-01
ST = 8.127754E+01 N/(mm^2)
SC = 3.449746E+02 N/(mm^2)
SS = 1.549405E+02 N/(mm^2)
Stress Strain Curve
Stress Type ENGINEERING
Pressure Constant = 1.800000E+00
Strain Rate = 0.000000E+00
Stress Cycle Curve
Stress Ratio = 1.000000E-01

Figure 131 Linear Matrix Properties

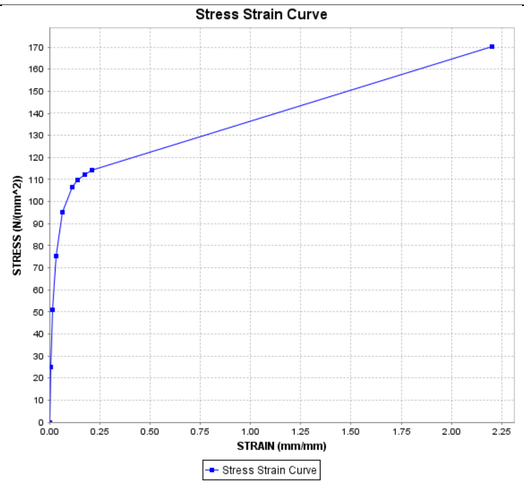

Figure 14 Non Linear SS Curve for Matrix

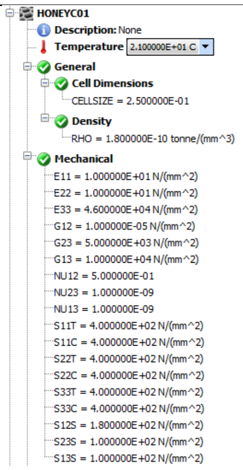

HONEYC01
Description: None
Temperature 2.100000E+01 C
General
Cell Dimensions
CELLSIZE = 2.500000E-01
Density
RHO = 1.800000E-10 tonne/(mm^3)
Mechanical
E11 = 1.000000E+01 N/(mm^2)
E22 = 1.000000E+01 N/(mm^2)
E33 = 4.600000E+04 N/(mm^2)
G12 = 1.000000E-05 N/(mm^2)
G23 = 5.000000E+03 N/(mm^2)
G13 = 1.000000E+04 N/(mm^2)
NU12 = 5.000000E-01
NU23 = 1.000000E-09
NU13 = 1.000000E-09
S11T = 4.000000E+02 N/(mm^2)
S11C = 4.000000E+02 N/(mm^2)
S22T = 4.000000E+02 N/(mm^2)
S22C = 4.000000E+02 N/(mm^2)
S33T = 4.000000E+02 N/(mm^2)
S33C = 4.000000E+02 N/(mm^2)
S12S = 1.800000E+02 N/(mm^2)
S23S = 1.000000E+02 N/(mm^2)
S13S = 1.000000E+02 N/(mm^2)

Figure 15 Honeycomb Properties

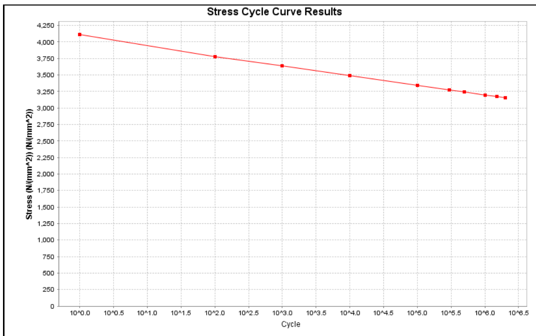

Figure 16 SN Curve for Fiber

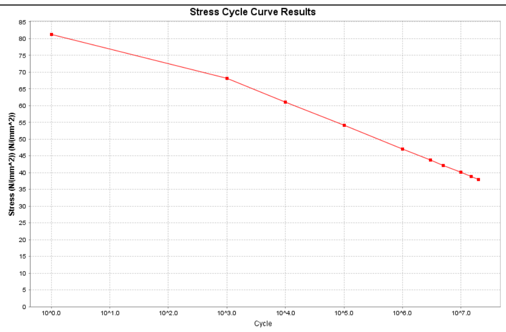

Figure 17 SN Curve for Matrix

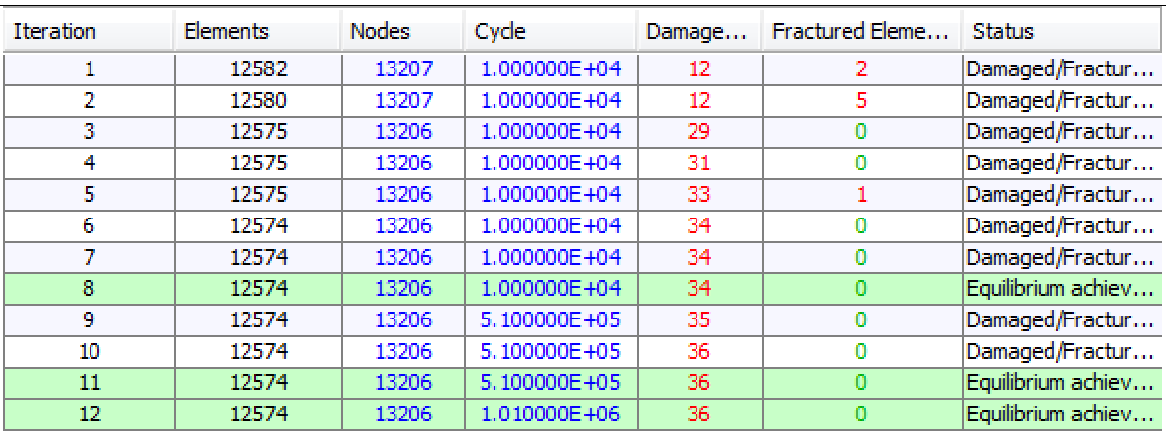

Iteration	Elements	Nodes	Cycle	Damage...	Fractured Eleme...	Status
1	12582	13207	1.000000E+04	12	2	Damaged/Fractur...
2	12580	13207	1.000000E+04	12	5	Damaged/Fractur...
3	12575	13206	1.000000E+04	29	0	Damaged/Fractur...
4	12575	13206	1.000000E+04	31	0	Damaged/Fractur...
5	12575	13206	1.000000E+04	33	1	Damaged/Fractur...
6	12574	13206	1.000000E+04	34	0	Damaged/Fractur...
7	12574	13206	1.000000E+04	34	0	Damaged/Fractur...
8	12574	13206	1.000000E+04	34	0	Equilibrium achiev...
9	12574	13206	5.100000E+05	35	0	Damaged/Fractur...
10	12574	13206	5.100000E+05	36	0	Damaged/Fractur...
11	12574	13206	5.100000E+05	36	0	Equilibrium achiev...
12	12574	13206	1.010000E+06	36	0	Equilibrium achiev...

Figure 18 Log of Iterations, Elements, Cycle No., Damaged Elements, and Fractured Elements

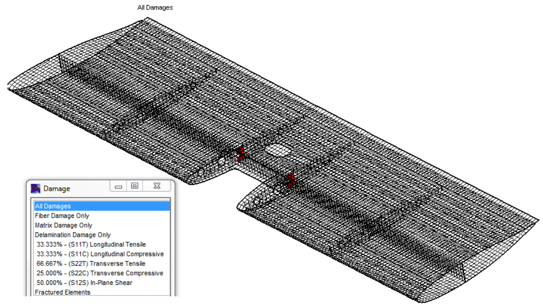

All Damages
Fiber Damage Only
Matrix Damage Only
Delamination Damage Only
33.333% - (S11T) Longitudinal Tensile
33.333% - (S11C) Longitudinal Compressive
66.667% - (S22T) Transverse Tensile
25.000% - (S22C) Transverse Compressive
50.000% - (S12S) In-Plane Shear
Fractured Elements

Figure 19 Damage Initiation at 1e04 cycles

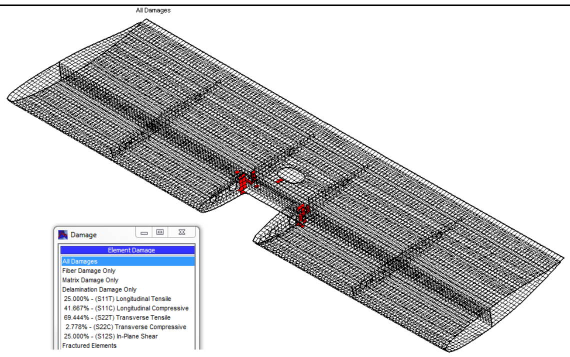

Element Damage
All Damages
Fiber Damage Only
Matrix Damage Only
Delamination Damage Only
25.000% - (S11T) Longitudinal Tensile
41.667% - (S11C) Longitudinal Compressive
69.444% - (S22T) Transverse Tensile
2.778% - (S22C) Transverse Compressive
25.000% - (S12S) In-Plane Shear
Fractured Elements

Figure 20 Damage Propagation at 2e07 cycles

4 RESULTS AND DISCUSSION

The first few iterations and number of damaged and fractures elements in the simulation are shown in Figure 18Figure.

Figure 19 and Figure 20 shows damage mechanisms for the horizontal tail. They are split up into matrix shear, matrix compression, matrix tension, and fiber failure. At times in fatigue, when damage occurs, material degradation softens the region and prevents other damages from happening. Here matrix tension and shear seems to have prevented much matrix compression from happening.

The starting cycle (blocks of spectrum loading) was 1e04 for the simulation and increased by 5e05 after that. If there is new damages or fracture, then the code attempts to reach equilibrium by decreasing the stiffness or removing elements, respectively. Damage initiation at 1e04 cycles and propagation at 2e07 cycles is shown in Figure 21 and Figure 22Figure. . They are shown to occur at the root of rib (section 3). Figure 22 shows layer matrix tension and fiber failure damages side by side within section 3 as shown by GENOA. A breakdown of the damage types in that region is shown in Figure 21. Finally, the locations within the layup and type of damages are shown in Figure 22.

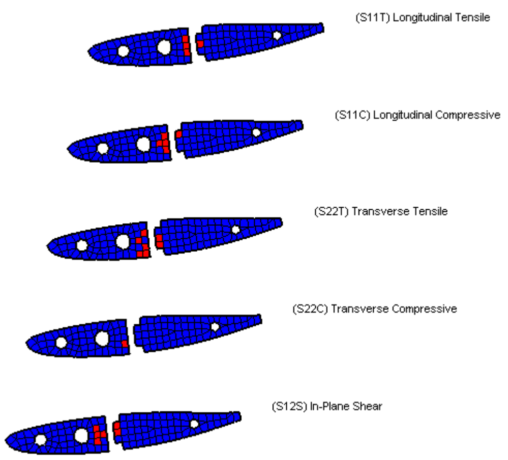

Figure 21 Several Damage Types in Rib at 2e07 cycles

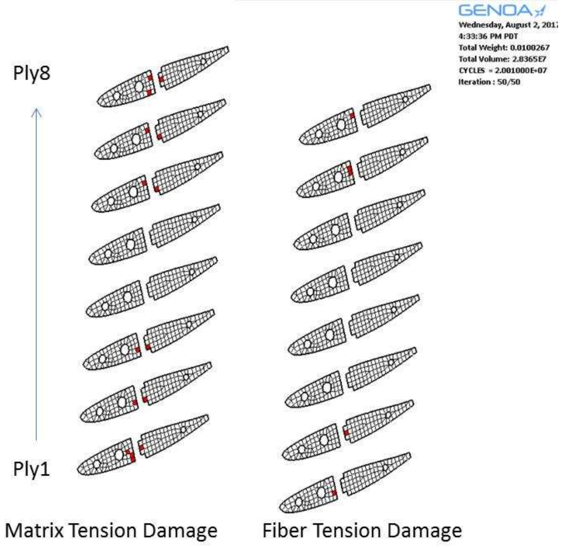

Figure 22 Ply Damages Located and Identified at 2e07 cycles

5 CONCLUSIONS

In this paper, a multi-scale progressive failure analysis of HT against fatigue spectrum loading is conducted. Simulation results show that this multi-scale progressive failure analysis captures: 1) all possible damage and fracture modes, 2) the type(s) of flaws initiating given fracture modes, and 3) the coalescing and propagation of flaws at critical locations for imminent structural failure. The simulation of the HT showed it to begin to have damage at 1e04 cycles of the block loading mentioned and in section 3 of the tail. There was fiber and matrix tension and compression damage as well as matrix shear. At 2e07 cycles, the damage propagated but not to a critical level. Investigation of the tensile damages at 2e07 blocks showed both matrix tension and fiber tension damage in the outer plies of Rib (section 3).

6 ACKNOWLEDGEMENTS

The views and conclusions contained in this article should not be interpreted as representing the official policies, either expressed or implied, of the Hindustan Aeronautics Limited.

7 REFERENCES

[1] Wöhler A., Über die Festigkeitsversuche mit Eisen und Stahl. Zeitschrift für Bauwesen 20:73–106, 1870.

[2] Damage Tolerance and Fatigue Evaluation of Composite Rotorcraft Structures. NPRM No. 09–12 (Notice of Proposed Rulemaking) for FAR 27/29.573 Federal Register, vol. 75(3), January 6, 2010.

[3] Bansemir, H., Mueller, R.: TheEC135–Applied Advanced Technology. In: AHS, 53rd Annual Forum, Virginia Beach, USA, April 29-May 1, 1997.

[4] Bansemir, H., Emmerling, S.: Fatigue Substantiation and Damage Tolerance Evaluation of Fibre Composite Helicopter Components. In: Applied Vehicle Technology Panel: Applications of Damage Tolerance Principles for Improved Airworthiness of Rotorcraft, Corfu, Greece, 1999.

[5] Miner M A., Cumulative damage in fatigue. Trans ASME J Appl Mech 12:A159–A164, 1945.

[6] Gassner E., Strength experiments under cyclic loading in aircraft structures. Luftwissen 6:61–64, 1939.

[7] Cody Godines, Saber DorMohammadi, Frank Abdi, Marc Villa Montero, Dade Huang, Levon Minnetyan, "Damage Tolerant Composite Design Principals for Aircraft Components Under Static Service Loading using Multi-Scale Progressive Failure Analysis" Journal of Composite Materials, Volume: 51 issue: 10, May 1, 2017.

[8] Saber DorMohammdi, Cody Godines, Frank Abdi, Dade Huang, Massimiliano Repupilli Levon Minnetyan, "Damage Tolerant Composite Design Principals for Aircraft Components Under Fatigue Service Loading Using Multi-Scale Progressive Failure Analysis". Journal of Composite Material, Volume: 51 issue: 15, June 1, 2017.

[9] Frank Abdi, Joshua Paquette, Glenn Crans, Levon Minnetyan, Pier Marzocca, "Durability of Tapered Composite Laminates under Static and Fatigue Loading", 52nd AIAA/ASME/ASCE/AHS/ASC Structures, Structural Dynamics and Materials Conference, 4 - 7 April 2011.

[10] Galib Abumeri, Joshua Paquette, Frank Abdi, "Durability and Reliability of Wind Turbine Composite Blades Using Robust Design Approach,", 52nd AIAA/ASME/ASCE/AHS/ASC Structures, Structural Dynamics and Materials Conference, 4 - 7 April 2011.

[11] Galib Abumeri and Frank Abdi, Joshua Paquette "Durability and Reliability of Large Wind Turbine Composite Blades". SAMPE 2012, Baltimore Conference Paper May 18-20, 2012.